

ChemComm

Accepted Manuscript



This article can be cited before page numbers have been issued, to do this please use: C. Wu, K. Wu, J. Liu, X. Zhou, C. Leung and D. Ma, *Chem. Commun.*, 2019, DOI: 10.1039/C9CC02189B.



This is an Accepted Manuscript, which has been through the Royal Society of Chemistry peer review process and has been accepted for publication.

Accepted Manuscripts are published online shortly after acceptance, before technical editing, formatting and proof reading. Using this free service, authors can make their results available to the community, in citable form, before we publish the edited article. We will replace this Accepted Manuscript with the edited and formatted Advance Article as soon as it is available.

You can find more information about Accepted Manuscripts in the [author guidelines](#).

Please note that technical editing may introduce minor changes to the text and/or graphics, which may alter content. The journal's standard [Terms & Conditions](#) and the ethical guidelines, outlined in our [author and reviewer resource centre](#), still apply. In no event shall the Royal Society of Chemistry be held responsible for any errors or omissions in this Accepted Manuscript or any consequences arising from the use of any information it contains.

COMMUNICATION

A dual-functional molecular strategy for in-situ suppressing and visualizing of neuraminidase in aqueous solution using iridium(III) complexes†

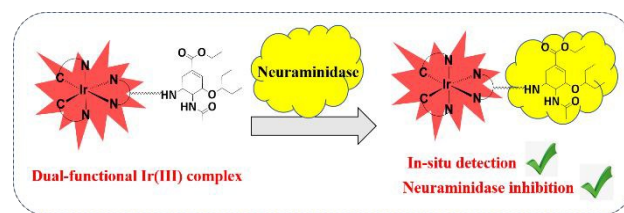
Received 00th January 20xx,
Accepted 00th January 20xxChun Wu,^{‡a} Ke-Jia Wu,^{‡b} Jin-Biao Liu,^{‡a,c} Xiao-Ming Zhou,^d Chung-Hang Leung^{*b} and Dik-Lung Ma^{*a}

DOI: 10.1039/x0xx00000x

We have designed for the first time a dual-functional luminescent probe and inhibitor of neuraminidase (NA), a key influenza target. The lead iridium(III) complex exhibited enhanced inhibition against NA compared to the FDA-approved antiviral drug, oseltamivir, and could detect NA even in the presence of an autofluorescent background.

Neuraminidase (NA) is a glycoprotein found on the surface of influenza viruses, and is crucial for enabling the release of newly generated viruses from infected host cells.¹ Hence, NA-targeting therapeutics are a primary strategy for combating influenza infection.² Officially approved NA-targeting drugs include peramivir, zanamivir and oseltamivir,³ with oseltamivir showing the greatest protection against influenza among the three. However, the rapid antigenic mutation rate of influenza viruses has fostered the emergence of resistance to current drugs, particularly to oseltamivir,⁴ creating a critical threat to influenza treatment. To date, various organic compounds have been explored for the inhibition of oseltamivir-resistant influenza viruses.⁵ However, one drawback of using organic compounds is their intrinsic fluorescence or quenching effects, which might lead to false positive or negative results when screening for NA inhibitors using fluorescence assays.⁶

Meanwhile, the development of rapid and reliable diagnostic platforms for influenza infection is urgently needed for the timely control and management of influenza infection. For example, the organic dye X-Neu5Ac has been designed as an imaging reagent for NA.⁷ The Suzuki group recently developed a more sensitive fluorogenic and precipitating imaging reagent, BTP-Neu5Ac, that has been used to visualize mammalian tissue sialidases, influenza virus NA and sialidase activity in several other viruses.⁸ Moreover, the Wong group



Scheme 1 Schematic diagram showing the in-situ tracking and suppressing of NA activity using an iridium(III)-based probe.

developed a fluorescent difluorosialic acid-based, cell-permeable probe to label and visualize a variety of human and influenza NAs.⁹ Recently, Withers and co-workers have developed an organic dye as a proximity ligation reagent to specifically detect influenza virus in mammalian cells.¹⁰ However, all organic dye-based probes share a common weakness of short-lived fluorescence, rapid photobleaching rates and negligible Stokes shift that can hinder their application for the real-time sensing of NA in biological situations.¹¹

The development of dual-function therapeutic and imaging molecules has received recent interest in the literature.¹² Combining a drug and a probe into a single molecular entity could facilitate the treatment of specific diseases while simultaneously allowing for the real-time and targeted tracking of the therapeutic efficiency, delivery kinetics, or trafficking pathways of the drug.¹³ Moreover, the need for an extraneous inhibitor or imaging agent is eliminated, which simplifies administration and eliminates the potential for undesirable drug-drug interactions.¹⁴ However, no example of dual-function inhibitors and probes for NA have been reported yet.

One great challenge in the design of a dual-functional inhibitor and probe for NA is how to achieve the desired activity and selectivity for NA whilst simultaneously maintaining sufficient photophysical activity in an aqueous environment. Transition metal complex-based scaffolds enjoy distinct advantages as bio-sensing and chemo-sensing agents over organic molecules owing to their unique characteristics,¹⁵ including large Stokes shift, high luminescent quantum yield, long-lived phosphorescent lifetime, high sensitivity of emission characteristics to subtle variations from chemical environment, and modular synthesis that enables the efficient production of analogues with variable photophysical and/or chemical properties.¹⁶ Typically, transition metal complex-based

^a Department of Chemistry, Hong Kong Baptist University, Kowloon, Hong Kong, China. E-mail address: edmondma@hkbu.edu.hk (Dik-Lung Ma).

^b State Key Laboratory of Quality Research in Chinese Medicine, Institute of Chinese Medical Sciences, University of Macau, Macao, China. E-mail address: duncanleung@um.edu.mo (Chung-Hang Leung).

^c School of Metallurgical and Chemical Engineering, Jiangxi University of Science and Technology, Ganzhou, China.

^d MOE Key Laboratory of Laser Life Science and Institute of Laser Life Science, College of Biophotonics, South China Normal University, Guangzhou, China.

‡ The authors contribute equally in this work.

* Corresponding authors.

† Electronic Supplementary Information (ESI) available.

ARTICLE

luminescent probes employ either “always-on”, “switch-on” or “switch-off” signaling modes after interaction with the target analyte.¹⁷ Always-on or switch-on probes display high target-to-background ratios by emitting continuous or enhanced luminescence in the presence of analyte, allowing their signals to distinguished in the presence of complicated biological interferences. On the other hand, the switch-off signaling mode can be susceptible to interference by non-specific quenchers in the cellular environment. Hence, always-on or switch-on probes are highly preferred for the real-time monitoring of targeted analytes in living systems.¹⁸ On the basis of our current research interest in metal complex-based luminescent probes, we aimed to develop a series of new oseltamivir-conjugated iridium(III) complexes for the selective inhibition and detection of NA (Scheme 1). Specifically, the assembled probes consist of an oseltamivir “binding unit”, which is responsible for the selectivity and binding affinity of the probe towards NA, conjugated to an iridium(III) “signaling unit”. Upon selective binding of the probe to NA, the distinguished luminescence emission from the iridium(III) signaling moiety allows for the dynamic tracing of NA. Meanwhile, the introduction of the oseltamivir moiety is expected to confer NA inhibitory activity,¹⁹ allowing the probe to also function as a potential therapeutic agent for treating influenza infection. Our molecular design of the complexes also takes into account the emissive behavior of the cyclometalated metal complex moiety. Most transition metal complexes display weak emission in aqueous solutions,²⁰ which greatly limits their application for sensing in the biological environment. Moreover, red-emitting probes are generally more desirable since they are less susceptible to interference by optical absorption, light scattering and autofluorescence of biological issues.²¹ Hence, our ultimate design goal was to develop NA-selective iridium(III) complexes with strong red emission in aqueous condition.

In this study, four kinds of C^N ligands and two kinds of N^N ligands were conjugated to the iridium(III) metal core. The small library of iridium(III) complexes have been designed by varying the auxiliary ligands in order to fine-tune their photophysical and physicochemical properties, such as emission wavelength, phosphorescent lifetime, Stokes shift and quantum yield. The final complexes **1a–1d** all contain an oseltamivir moiety grafted onto the N^N ligand of the parent iridium(III) scaffold.

To synthesize the dual-functional iridium(III) complexes, oseltamivir phosphate **2** was initially attached to the N^N ligand through two different strategies, either starting from the amine-containing 1,10-phenanthroline-5-amine (Synthesis Route 1, Scheme S1), or the more reactive carboxyl-containing 1,10-phenanthroline-5-carboxylic acid (Synthesis Route 2, Scheme S1). Unfortunately, the yield of the targeted oseltamivir conjugates **5** or **8** was low owing to the poor solubility of oseltamivir phosphate **2** in organic solvent. To overcome this, oseltamivir phosphate **2** was first transformed into the organic solvent-soluble oseltamivir trifluoroacetate **10** (Scheme S2). However, conjugation of oseltamivir trifluoroacetate **10** to the N^N ligand 1,10-phenanthroline-5-carboxylic acid proceeded poorly (Synthesis Route 3, Scheme S1).

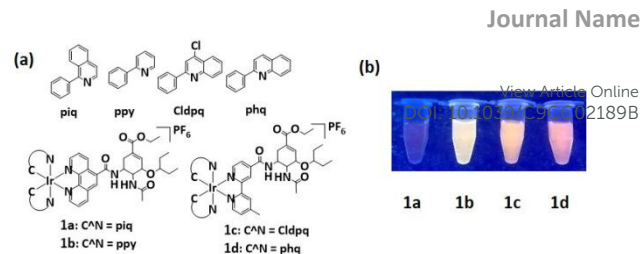


Fig. 1 (a) Chemical structures of iridium(III) complexes **1a–1d**. (b) Photographs of complexes **1a–1d** (2.5 μM) observed under UV light (365 nm) in PBS buffer containing 0.5% ACN.

Instead, we found that **10** could be directly conjugated to the cyclometalated iridium(III) complex precursor **11a** already bearing the 1,10-phenanthroline-5-carboxylic acid N^N ligand under standard EDCI/HOBT coupling conditions, producing the final oseltamivir-conjugated compound **1a** (Fig. 1a) in 62% yield. The parent iridium(III) complex precursor **11a** was synthesized by the reaction of 1,10-phenanthroline-5-carboxylic acid with the dichloro-bridged dimer **7**, which was in turn synthesized from the C^N ligand **6** and iridium(III) chloride. The iridium(III) analogues **1b–1d** were prepared in similar fashion via the intermediate parent complexes **11b–11d**. Complexes **1a–1d** were fully characterized by high-resolution mass spectrometry (HRMS), ¹H NMR, ¹³C NMR and high performance liquid chromatography (HPLC) (Fig. S1). Remarkably, complexes **1a–1d** displayed strong luminescence in aqueous PBS buffer containing 0.5% ACN (Fig. 1b), which endows with the potential to function as dual-functional inhibitor and probes for NA.

We first studied the NA inhibition activity of the novel oseltamivir-conjugated complexes **1a–1d** using a fluorescence assay (Fig. 2). Encouragingly, complexes **1a–1d** (100 μM) showed significant inhibition of NA activity compared to the DMSO control. Notably, complexes **1a–1d** all showed superior inhibition activity over the reference drug oseltamivir under the same *in-vitro* experimental conditions. This result suggests that the combination of the oseltamivir moiety and iridium(III) core and generate molecules with promising potential for treating influenza infection. In light of the unique optical properties of iridium(III) complexes, we next investigated the photophysical properties of complexes **1a–1d** (Table S1). In acetonitrile (ACN), complexes **1a–1d** displayed characteristic absorbance bands at 210–288 nm in the UV-Vis spectra (Fig. S2a). Complexes **1a–1d** also exhibited maximum excitation and emission wavelengths at 354–381 nm and 585–606 nm, respectively, in PBS buffer containing 0.5% ACN (Fig. S2b), giving large Stokes shifts of 225–249 nm. Noticeably, complex **1d** exhibited the largest Stokes shift for 249 nm, which is much larger than the typical small Stokes shift of organic dyes at around 100 nm, thus giving it a great advantage in terms of preventing self-quenching.²²

Red luminescence is generally more desirable because of its superior penetration of biological cells and tissues.²³ Complexes **1b** and **1c** exhibited yellow to orange luminescence in PBS buffer, while complexes **1a** and **1d** displayed a red-shifted red luminescence at around 600 nm under the same aqueous condition. Interestingly, complex **1c** showed around 6-fold higher emission intensity compared to complexes **1a**, **1b** and **1d**. This might be attributed to the change of the metal-to-ligand-

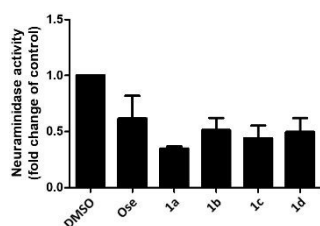


Fig. 2 Inhibition activity of complexes **1a–1d** and oseltamivir (Ose) (100 μM) against NA (10 $\mu\text{g}/\text{mL}$) as measured by a fluorescence assay. The fluorescence intensity was detected at $\text{ex}/\text{em} = 330 \text{ nm}/450 \text{ nm}$.

charge–transfer (MLCT) state and increased electron density induced by the joint interplay of the electron–withdrawing chloride moiety and the π – π conjugation system located in the auxiliary C^N and N^N ligands of **1c**. Additionally, all four complexes showed higher quantum yields than Ru(bpy)₃ (bpy = 2,2'-bipyridine), a commonly used transition metal complex standard with quantum yield at 0.062 (Fig. S2c). Finally, complexes **1a–1d** displayed long-lived phosphorescence lifetimes of ca. 0.277–0.565 μs (Fig. S2d), which is significantly longer than the typical nanosecond lifetimes of organic fluorophores. This characteristic could allow the emission of complexes **1a–1d** to be discriminated from a highly auto-fluorescent background.

Inspired by the promising luminescent characteristics of complexes **1a–1d**, we studied their application as luminescent probes for NA imaging. Complexes **1a–1d** showed negligible changes in luminescence upon the addition of NA in PBS buffer containing 0.5% ACN (Fig. S3), suggesting that they could function as “always–on” probes for NA. To testify whether complexes **1a–1d** can selectively bind to NA, possibly via the oseltamivir–binding site, we performed a competition assay with complexes **1a–1d** with oseltamivir. Upon the pre-incubation of NA with oseltamivir (100 μM), complexes **1a–1c** showed negligible luminescence change (Fig. S3), suggesting that these complexes did not significantly interact with NA. However, a significant decrease of the luminescence of complex **1d** was recorded when NA was pre-incubated with oseltamivir (Fig. 3a). Complex **1d** showed no direct interaction with oseltamivir alone in the absence of NA (Fig. 3b), suggesting that the decrease of luminescence intensity observed in the competition assay was due to competition at the oseltamivir–binding site of NA rather than through probe–probe interactions. Moreover, a protein thermal shift assay was performed to evaluate the binding affinity of complex **1d** with NA (Fig. 3c). Complex **1d** showed dose-dependent thermal stabilization of NA *in vitro*, with an apparent K_d of $18.95 \pm 0.04 \mu\text{M}$. To obtain the optimal performance of the probe, conditions such as pH and the nature of the buffer solution were optimized. As NA shows the highest activity at pH 5,²⁴ we explored the effect of pH in the range of pH 4–6 on the NA sensing activity of **1d**. The luminescence intensity of complex **1d** was robust in the absence (Fig. S4a) or presence (Fig. S4b) of NA in PBS buffer over the pH range from 4–6. Hence, a pH value of 5 was chosen for further investigation to preserve the highest biological activity of NA. Moreover, the effect of various buffer systems on the sensing performance of complex **1d** was also

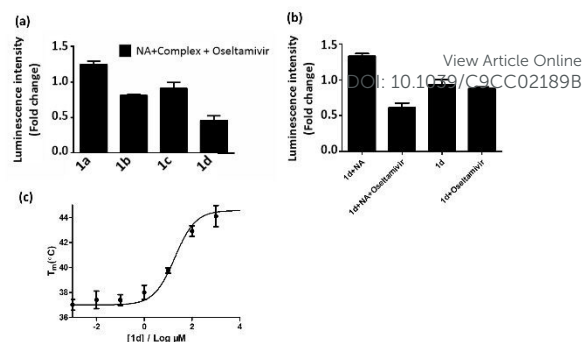


Fig. 3 (a) Competition assay of complexes **1a–1d** (100 μM) with oseltamivir (Ose) (100 μM) for NA (10 $\mu\text{g}/\text{mL}$) detection. The luminescence intensity of the mixture of NA and complex was utilized as control respectively. (b) Luminescence intensity of complex **1d** in the absence or presence of oseltamivir (Ose) (100 μM) or NA (10 $\mu\text{g}/\text{mL}$). The luminescence intensity was detected at $\text{ex}/\text{em} = 330 \text{ nm}/600 \text{ nm}$. (c) Interaction of NA with **1d** as measured by a protein thermal shift assay.

explored. The data showed that PBS (containing 0.5% ACN) gave a slightly higher luminescent enhancement in response to NA compared to the use of Tris–HCl or HEPES buffer systems (Fig. S4c). Therefore, PBS buffer was used for further experiments. Under the optimized conditions, the luminescence response of complex **1d** towards different concentrations of NA was tested. The luminescence of **1d** gradually increased with increasing concentration of NA from 1–20 $\mu\text{g}/\text{mL}$, with a detection limit at 0.68 $\mu\text{g}/\text{mL}$, indicating that **1d** allows for NA detection in a concentration–dependent manner (Fig. S5).

To verify that the luminescence of complex **1d** could be maintained in the cellular environment, complex **1d** was challenged with various potentially interfering species, including 20 common amino acids, glutathione (GSH), glutathiol (GSSG), homocysteine, homocysteine, S₂[–], HCO₃[–], CO₃^{2–}, SO₃^{2–}, Br[–], Cl[–], SO₄^{2–}, F[–], ClO₄[–], NO₃[–], HPO₄^{2–}, H₂PO₄[–], I[–], CH₃COO[–], Mg²⁺, Fe³⁺, Cd²⁺, Ag⁺, Ni²⁺, Pb²⁺, Ba²⁺, Cu²⁺, Al³⁺, Na⁺, K⁺, Ca²⁺, Zn²⁺, Fe²⁺ and Mn²⁺ (Fig. S6). The results revealed that complex **1d** could maintain robust luminescence in the presence of the various interfering species. Next, we measured the emission of **1d** using time–resolved emission spectroscopy (TRES). The fluorescent organic dyes thioflavin S (THS) and coumarin 460 (Cm460) were used as model matrix interferences. In steady–state emission mode, the emission of complex **1d** was perturbed by the strong emission peak of THS and Cm460 at 428 nm and 460 nm respectively (Fig. S7a), leading to reduced accuracy in the measurement of NA concentration. However, when the time gate was defined as after the completion of the fluorescence decay of THS and Cm460, the interfering signals from THS and Cm460 were almost completely lost and only the emission of complex **1d** was observed (Fig. S7b). These results demonstrate the potential utilization of the long–lived **1d** in highly auto–fluorescent environments using TRES.

As the complex with the highest binding affinity to NA, complex **1d** was therefore chosen as the most promising dual–function agent. The biological potency of **1d** was subsequently assessed using a dose–response experiment with various concentrations of complex **1d**. With increasing concentration of complex **1d** (10–200 μM) as inhibitor, the activity of NA was gradually reduced with IC₅₀ at around 20 μM , indicating that

complex **1d** inhibited the NA activity in a dose-dependent manner (Fig. S8).

In conclusion, using a structure-based molecular design strategy, we have for the first time successfully developed a dual-functional Iridium(III) complex-based platform for in-situ suppressing and visualizing of NA under aqueous conditions. In terms of the inhibition properties, complexes **1a–1d** showed superior inhibition efficiency compared to the FDA-approved NA inhibitor oseltamivir under the same experimental conditions. Notably, complex **1d** also displayed promising potential as an “always-on” luminescent probe for NA due to its long-lived lifetime, large Stokes shift, high quantum yield and strong red emission in aqueous PBS buffer containing 0.5% ACN. Moreover, complex **1d** also enables the dose-dependent detection of NA with high selectivity at 0–20 µg/mL. In summary, complex **1d** is the first highly promising transition metal-based dual-functional candidate for the in-situ monitoring and inhibition of NA. We envision that complex **1d** can facilitate a new route for developing real-time and in-field assessment tools against targeted biomarkers for guided therapy for influenza viruses.

This work is supported by Hong Kong Baptist University (FRG2/16-17/007 and FRG2/17-18/003), the Health and Medical Research Fund (HMRF/14150561), the Research Grants Council (HKBU/12301115), the National Natural Science Foundation of China (21575121, 21775131, 21628502 and 21762018), the Hong Kong Baptist University Century Club Sponsorship Scheme 2018, the Interdisciplinary Research Matching Scheme (RC-IRMS/16-17/03), Interdisciplinary Research Clusters Matching Scheme (RC-IRCS/17-18/03), Matching Proof of Concept Fund (MPCF-001-2017/18), Collaborative Research Fund (C5026-16G), SKLEBA and HKBU Strategic Development Fund (SKLP_1718_P04), the Science and Technology Development Fund, Macao SAR (077/2016/A2), and the University of Macau (MYRG2016-00151-ICMS-QRCM and MYRG2018-00187-ICMS).

Conflicts of interest

There are no conflicts of interest to declare.

Notes and references

- R. J. Russell, L. F. Haire, D. J. Stevens, P. J. Collins, Y. P. Lin, G. M. Blackburn, A. J. Hay, S. J. Gamblin and J. J. Skehel, *Nature*, 2006, **443**, 45.
- A. Lackenby, T. G. Besselaar, R. S. Daniels, A. Fry, V. Gregory, L. V. Gubareva, W. Huang, A. C. Hurt, S.-K. Leang and R. T. Lee, *Antiviral Res.*, 2018, **157**, 38.
- J. Wang, C. Ma, J. Wang, H. Jo, B. Canturk, G. Fiorin, L. H. Pinto, R. A. Lamb, M. L. Klein and W. F. DeGrado, *J. Med. Chem.*, 2013, **56**, 2804.
- E. Takashita, A. Meijer, A. Lackenby, L. Gubareva, H. Rebelo-de-Andrade, T. Besselaar, A. Fry, V. Gregory, S.-K. Leang and W. Huang, *Antiviral Res.*, 2015, **117**, 27.
- S. Chamni and W. De-Eknamkul, *Expert. Opin. Ther. Pat.*, 2013, **23**, 409.
- J. Kongkamnerd, A. Milani, G. Cattoli, C. Terregino, I. Capua, L. Beneduce, A. Gallotta, P. Pengo, G. Fassina and O. Monthakantirat, *J. Biomol. Screen.*, 2011, **16**, 755.
- M. Saito, H. Hagita, Y. Iwabuchi, I. Fujii, K. Ikeda and M. Ito, *Histochem. Cell Biol.*, 2002, **117**, 453. DOI: 10.1039/C9CC02189B
- (a) A. Minami, T. Otsubo, D. Ieno, K. Ikeda, H. Kanazawa, K. Shimizu, K. Ohata, T. Yokochi, Y. Horii and H. Fukumoto, *PLoS One*, 2014, **9**, e81941; (b) Y. Kurebayashi, T. Takahashi, T. Otsubo, K. Ikeda, S. Takahashi, M. Takano, T. Agarikuchi, T. Sato, Y. Matsuda and A. Minami, *Sci. Rep.*, 2014, **4**, 4877.
- C.-S. Tsai, H.-Y. Yen, M.-I. Lin, T.-I. Tsai, S.-Y. Wang, W.-I. Huang, T.-L. Hsu, Y.-S. E. Cheng, J.-M. Fang and C.-H. Wong, *Proc. Nat. Acad. Sci. USA*, 2013, **110**, 2466.
- Z. Gao, A. J. Thompson, J. C. Paulson and S. G. Withers, *Angew. Chem. Int. Edit.*, 2018, **130**, 13726.
- K. Vellaisamy, G. Li, W. Wang, C.-H. Leung and D.-L. Ma, *Chem. Sci.*, 2018, **9**, 8171.
- (a) Q. Wang, R. Chaerkady, J. Wu, H. J. Hwang, N. Papadopoulos, L. Kopelovich, A. Maitra, H. Matthaei, J. R. Eshleman and R. H. Hruban, *Proc. Natl. Acad. Sci. USA*, 2011, **108**, 2444; (b) P. Shi, E. Ju, Z. Yan, N. Gao, J. Wang, J. Hou, Y. Zhang, J. Ren and X. Qu, *Nat. Commun.*, 2016, **7**, 13088; (c) N. Gao, H. Sun, K. Dong, J. Ren, T. Duan, C. Xu and X. Qu, *Nat. Commun.*, 2014, **5**, 3422; (d) C. Ouyang, L. Chen, T. W. Rees, Y. Chen, J. Liu, L. Ji, J. Long and H. Chao, *Chem. Commun.*, 2018, **54**, 6268.
- (a) H. M. Wahrenius, *Expert Opin. Med. Diagn.*, 2009, **3**, 381; (b) C. Vallotto, E. Shaili, H. Shi, J. S. Butler, C. J. Wedge, M. E. Newton and P. J. Sadler, *Chem. Commun.*, 2018, **54**, 13845; (c) C. A. Wootton, C. Sanchez-Cano, A. F. Lopez-Clavijo, E. Shaili, M. P. Barrow, P. J. Sadler and P. B. O'Connor, *Chem. Sci.*, 2018, **9**, 2733.
- (a) S. S. Kelkar and T. M. Reineke, *Bioconjug. Chem.*, 2011, **22**, 1879; (b) K. Y. Zhang, Q. Yu, H. Wei, S. Liu, Q. Zhao and W. Huang, *Chem. Rev.*, 2018, **118**, 1770; (c) K. Y. Zhang, T. Zhang, H. Wei, Q. Wu, S. Liu, Q. Zhao and W. Huang, *Chem. Sci.*, 2018, **9**, 7236.
- (a) W. Streciwilk, A. Terenzi, F. Lo Nardo, P. Prochnow, J. E. Bandow, B. K. Keppler and I. Ott, *Eur. J. Inorg. Chem.*, 2018, **2018**, 3104; (b) J.-J. Zhang, J. K. Muenzner, M. A. Abu el Maaty, B. Karge, R. Schobert, S. Wöfl and I. Ott, *Dalton Trans*, 2016, **45**, 13161; (c) Q. Chen, C. Jin, X. Shao, R. Guan, Z. Tian, C. Wang, F. Liu, P. Ling, J.-L. Guan, L. Ji, F. Wang, H. Chao and J. Diao, *Small*, 2018, **14**, 1802166.
- (a) G. J. Yang, W. Wang, S. W. F. Mok, C. Wu, B. Y. K. Law, X. M. Miao, K. J. Wu, H. J. Zhong, C. Y. Wong and V. K. W. Wong, *Angew. Chem. Int. Edit.*, 2018, **57**, 13091; (b) V. Rakers, P. Cadinu, J. B. Edell and R. Vilar, *Chem. Sci.*, 2018, **9**, 3459; (c) S. Bandeira, J. Gonzalez-Garcia, E. Pensa, T. Albrecht and R. Vilar, *Angew. Chem. Int. Ed. Engl.*, 2018, **130**, 316.
- H. Kobayashi and P. L. Choyke, *Acc. Chem. Res.*, 2011, **44**, 83.
- (a) K. Vellaisamy, G. Li, W. Wang, C.-H. Leung and D.-L. Ma, *Chem. Sci.*, 2018, **9**, 8171; (b) T.-H. Kwon, J. Kwon and J.-I. Hong, *J. Am. Chem. Soc.* 2008, **130**, 3726.
- K. Thorlund, T. Awad, G. Boivin and L. Thabane, *BMC Infect Dis*, 2011, **11**, 134.
- S. Arounaguiri and B. G. Maiya, *Inorg. Chem.*, 1999, **38**, 842.
- K. Y. Pu, K. Li and B. Liu, *Adv. Funct. Mater.*, 2010, **20**, 2770.
- T. He, Y. Wang, X. Tian, Y. Gao, X. Zhao, A. C. Grimsdale, X. Lin and H. Sun, *Appl. Phys. Lett.*, 2016, **108**, 011901.
- V. J. Pansare, S. Hejazi, W. J. Faenza and R. K. Prud'homme, *Chem. Mater.*, 2012, **24**, 812.
- G. Bahrami, B. Mohammadi and A. Kiani, *J. Chromatogr. B.*, 2008, **864**, 38.